Evaluating Riparian Vegetation Roughness Computations in the One-Dimensional HEC-RAS–RVSM Model

Zhonglong Zhang, PhD, PE, PH, Research Professor, Department of Civil and Environmental Engineering, Portland State University, Portland, OR 97207, e-mail: zz3@pdx.edu

Abstract

From the immense body of vegetative roughness literature, eleven computation equations have emerged with generic applicability and incorporated into the riparian vegetation module (RVSM) coupled with the one-dimensional HEC-RAS model. To evaluate the performance and applicability of eleven vegetation roughness equations, the HEC-RAS-RVSM model was applied to predict river stages of the San Joaquin River reach with dense and diverse riparian vegetation. Among eleven roughness equations, the Freeman et al. clearly overestimates the Manning's *n* values for the flow depth greater than its original experimental flow depth (1.5m). Whittaker et al. (2015) considers the reconfiguration of flexible vegetation and uses measured vegetation projected area, resulting in slightly more accurate prediction of river stage than all of the other equations. The equations of Baptist et al. (2007), Huthoff et al. (2007), and Cheng (2011), which modeled vegetation as rigid cylinders, produce identical and reasonable prediction of the river stage. Järvelä (2004) includes the impact of velocity on vegetation roughness and uses an indirect metric leaf area index to represent vegetation projected area, producing similar river stage prediction as the other equations based on a rigid cylinder analogy. Compared with manually calibrated Manning's *n*, the HEC-RAS–RVSM model with vegetation roughness equations is able to predict observed river stage, and performs particularly better for the flows exceeding the maximum calibration flow. The present study also demonstrates that the equations modeled vegetation as rigid cylinders are applicable for computing dynamic *n* values in 1D hydraulic simulation for the areas where most of the riparian vegetation is not fully submerged and dominated by trees and shrubs.

Introduction

Riparian vegetation on the floodplains has significant ecological functions in providing critical habitat, stabilizing the river bank and improving water quality through intercepting nutrients and contaminants (Naiman, 2005). On the other hand, vegetation increases local hydraulic roughness, exert additional drag force and thus may intensify flooding (Augustijn et al., 2008; Luhar and Nepf, 2013; Stone et al., 2013). The trade-off between flood and ecological management underlines a need to predict dynamic channel resistance and vegetation Manning's roughness coefficient (*n*) values in river hydraulic modeling studies. Vegetation roughness is generally spatially and temporally dynamic and is highly dependent on the distribution and physical properties of vegetation as well as hydraulic conditions such as flow depth and velocity (Acrement and Schneider, 1989; De Doncker, 2009). In river hydraulic modeling, it has always been a challenge to calibrate and determine hydraulic roughness resulting from riparian vegetation (Stone et al., 2013).

A large number of numerical equations have been developed to estimate hydraulic roughness of vegetated rivers in terms of Manning's *n*. Hession and Curran (2013) provide a comprehensive

literature review of trends and research in the topic of vegetation-induced roughness in fluvial systems. From the immense body of vegetative roughness literature, eleven roughness quantitative equations listed in Table 1 have emerged with generic applicability. Some of these equations are developed based on laboratory or field experiments (Wu et al., 1999; Freeman et al., 2000). Most equations (Fischenich, 2000; Järvelä, 2004; Baptist et al., 2007; Huthoff et al., 2007; Cheng, 2011; Luhar and Nepf, 2013; Whittaker et al., 2015) are theoretically derived from the force balance of a control volume of water in which gravitational force in the flow direction is equal to the drag force of vegetation and of the bed. For simplicity, Baptist et al. (2007), Huthoff et al. (2007), and Cheng (2011) modeled vegetation plants as uniformly distributed rigid cylinders. The flow resistance of leaves and branches is neglected and only resistance of stems is taken into account in their equations. Theoretically, these equations are applicable for trees and shrubs with few leaves and branches or for leaves and branches that are not submerged. Järvelä (2004) introduced a stream ordering scheme into trees to estimate the frontal area of stems and branches for leafless trees and shrubs. Fischenich (2000) and Whittaker et al. (2015) included a measured frontal projected area of the vegetation. Järvelä (2004) and Jalonen et al. (2013) used leaf area index (LAI) as an alternative to the frontal projected area. Järvelä (2004) and Whittaker et al. (2015) introduced the Vogel exponent, ψ, of velocity into their drag force equations. Additional mechanical properties of vegetation were included into equations of Freeman et al. (2000), Kouwen and Fathi-Moghadam (2000), Whittaker et al. (2015), and Kouwen and Li (1980).

Table 1. Vegetation roughness equations and associated parameters

Roughness equation	Suitability	Physical property of vegetation						Hydraulic metrics			Parameters	
		Plant density	Plant height	Stem diameter	Canopy height & width	Stiffness	LAI	Depth	Velocity	Energy slope	Drag coeff	Vogel exp
Huthoff et al., 2007	Tree, shrub	√	√	√				√			√	
Cheng, 2011	Tree, shrub	√	√	√				√			√	
Baptist et al., 2007	Tree, shrub	√	√	√				√			√	
Järvelä, 2004 (leafy)	Emergent tree, shrub		√				√	√	√		√	√
Järvelä, 2004 (leafless)	Emergent tree, shrub	√	√	√				√				
Freeman et al., 2000	Tree, shrub	√	√		√	√ (E_s)		√		√		
Fischenich, 2000	Tree, shrub	√	√	√	√			√			√	
Kouwen and Fathi-Moghadam, 2000	Emergent conifer trees		√			√ (ξE)		√	√			
Luhar and Nepf, 2013	Emergent tree, shrub	√	√	√	√			√			√	
Whittaker et al., 2015	Emergent tree, shrub	√	√	√	√	√ (EI)		√	√		√	√
Kouwen and Li, 1980	Submerged grass		√			√ (MEI)		√		√		
n-UR	Submerged grass		√					√	√			

The vegetation roughness qualitative equations listed in Table 1 were integrated into HEC-RAS – RVSM model to compute spatially and temporally varying Manning's *n* values in hydraulic simulations. The applicability and performance of these equations in HEC-RAS – RVSM model was evaluated through the San Joaquin River case study.

Methodology

HEC-RAS–RVSM Model

The eleven vegetation roughness equations were incorporated in HEC-RAS–RVSM for computing varying Manning's *n* values in hydraulic simulations (Zhang et al. 2019). Given that the Manning's *n* values are defined at the river cross section in the 1D hydraulic model, the hydraulic model domain is first discretized into rows of slice polygons that are centered on cross sections. The number of slice polygons along the cross section is defined according to the spatial heterogeneity of local vegetation and cross-section geometry. A high-resolution polygon mesh is necessary where either river bottom is steep or vegetation distribution changes. Initial riparian vegetation information is mapped to the cross-section slice polygons through the overlay of cross-section slice polygons and vegetation mapping. The 1D HEC-RAS model computes flow depth, velocity, and energy slope for the cross section slice polygon, which are directly used in above roughness equations to estimate Manning's *n* values. In turn dynamically computed Manning's *n* values are fed back into the 1D HEC-RAS model. In HEC-RAS, computed Manning's *n* can be updated at the user defined time step during the simulation.

Riparian vegetation along the river is often diverse, probably with grass or forest on the upland and willow or cottonwood at the water's edges. Flow depth and velocity along the river cross section are also varying. The diverse vegetation distribution and flow conditions can result in highly varying Manning's *n* values within a cross section. If multiple vegetation types coexist within the cross-section slice polygon, Manning's *n* values are first computed for each vegetation type. After Manning's *n* for riparian vegetation is computed, it is added to the user-defined Manning's *n* value for bare river bed to obtain the total Manning's *n* value of the cross-section using the equation given by Acrement and Schneider (1989) and Wu (2007):

$$n = \sqrt{n_v^{\,2} + n_b^2}\,, \qquad n_v = \sqrt{\sum_{i=1}^{k} n_i^{\,2}}$$

where n is the total Manning's n value for a cross-section; and n_b is the Manning's n value for the bare river bed, n_v is the combined Manning's n value of all the vegetation types within the cross-section slice polygon; i is the ith vegetation type; n_i is Manning's n value of the ith type; and k is the total number of vegetation types.

Application and Evaluation of HEC-RAS–RVSM

Study Site:

A reach of the San Joaquin River below Friant Dam from Highway 99 to Gravelly Ford near Fresno, California (Figure 1) was chosen to evaluate the feasibility of computing dynamic Manning's *n* values in modeling vegetated channels. This reach extends 25.7 km with dense and diverse native riparian vegetation. Typical riparian vegetation communities of the southwest USA such as cottonwood forest, willow forest, oak forest, riparian scrub are distributed along this river reach (Moise and Hendrickson, 2002). As a portion of the San Joaquin River restoration program, this reach has abundant hydraulic and vegetation data available for studying riparian vegetation's impact on river hydraulics. Three hydrologic stations have been installed and operated from the early 2000s, namely Donny Bridge (DNB), Skaggs Bridge (SKB), Gravelly Ford (GRF). USGS gage station No. 11251000 (below Friant Dam) is located approximately 40 km upstream of this reach. The flows of the study reach were observed to be low and stable due to the regulation of the upstream Friant Dam. Large flood events (above 200

m^3/s) occurred only in 2005, 2006, 2011 and 2017 since the establishment of the first hydrological station GRF in 2002. Water losses due to infiltration, evaporation and diversion were observed for the reach (Tetra Tech, 2013).

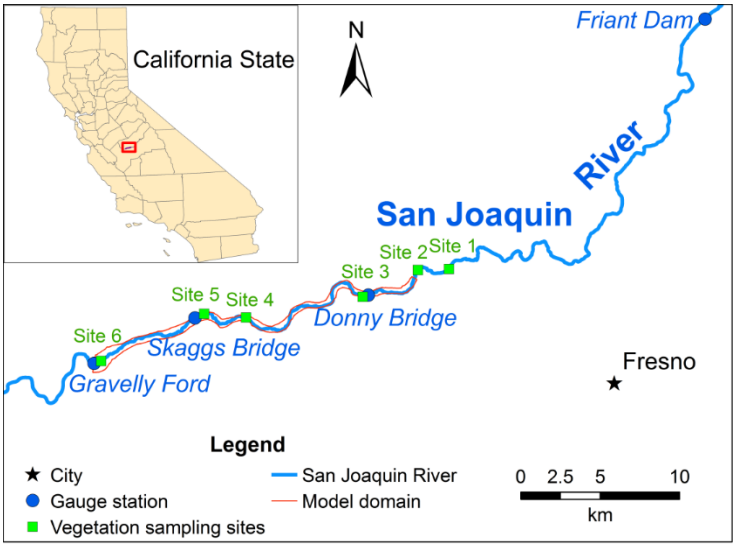

Figure 1. Study reach of the San Joaquin River

2002's vegetation map was used to represent initial spatial distribution of the vegetation communities. Previous research (Moise and Hendrickson, 2002) classified the riparian vegetation of the study reach into 28 vegetation communities based on a modified Holland system (Holland, 1986) and the work of Hink and Ohmart (1984). Six vegetation types, e.g. cottonwood riparian, mixed riparian, willow riparian/scrub, riparian scrub, invasive giant reed and herbaceous were identified from these vegetation communities. Physical properties of each vegetation community were surveyed at six sites in 2013. The measured parameters included vegetation height, stem diameter, density, and LAI. Other vegetation parameters including modulus of plant stiffness, *E*, flexural rigidity, *EI*, were not measured in the field study, their values were obtained from the literature.

Model Development and Calibration:

In the San Joaquin River HEC-RAS–RVSM model, the *n-UR* curve was used to compute Manning's *n* values for herbaceous. Seven equations for trees and shrubs were used to compute the *n* values for cottonwood, mixed riparian, willow riparian, riparian scrub and giant reed. The parameters used in the seven roughness equations were calibrated against observed river stage profiles under six flow scenarios of 2011. The six flow scenarios cover a wide range of flow rates from 16.03 to 201.62 m^3/s. Each scenario was run as an independent unsteady flow simulation using a constant discharge as upstream boundary. Uniform lateral flow was included to take account of the observed water loss of the reach.

The species-dependent parameters in each vegetation roughness equation were calibrated to obtain the *best match* possible between modeled and observed profiles under all of the six flow scenarios. During the model calibration, the vegetation parameter values provided in the original roughness equation were always used as a starting point, drag coefficients were generally the primary calibration parameters while the values of Vogel exponent and reference velocity were mostly kept consistent with the original studies. The final calibration values of species-dependent parameters used in the vegetation roughness equations are given in Table 2. In addition, Manning's *n* value of the bare river bed was set to 0.035 $s/m^{1/3}$ for the entire reach

except a portion of the upper reach with 0.05 s/m$^{1/3}$. Since the vegetation field survey did not include agricultural land, river wash and disturbed, constant Manning's *n* values were applied: *n* = 0.045 s/m$^{1/3}$ for agricultural land, *n* = 0.03 s/m$^{1/3}$ for river wash, and disturbed, which is based on the calibration study of Gillihan (2013).

Table 2. Species-dependent parameter values in six vegetation roughness equations

Roughness equations	Vegetation type	Drag coefficient C_d	Vogel exponent ψ	Reference velocity U_χ (m/s)
Baptist et al., 2007;	cottonwood	0.5	-	-
Huthoff et al., 2007;	mixed riparian	0.7	-	-
Cheng, 2011;	willow riparian	0.5	-	-
Luhar and Nepf, 2013	riparian scrub	0.5	-	-
	arunda donax	0.5	-	-
Järvelä, 2004 (leafy)	cottonwood	0.1	-1	0.1
	mixed riparian	0.24	-0.5	0.1
	willow riparian	0.2	-1	0.1
	riparian scrub	0.2	-1	0.1
	arunda donax	0.2	-1	0.1
Whittaker et al., 2015	cottonwood	0.76	-0.8	-
	mixed riparian	0.99	-0.6	-
	willow riparian	0.88	-0.81	-
	riparian scrub	0.88	-0.81	-
	arunda donax	0.88	-0.81	-

Note: C_b in the equation of Baptist et al. (2007) was set to a large value i.e. 1000 to eliminate the contribution of river bed resistance to vegetation roughness.

Figure 2 compares river stage profiles predicted by the San Joaquin River HEC-RAS model with dynamically computed Manning's *n* values and observed data under the six calibration flow scenarios. The model with Manning's *n* computed by Freeman et al. (2000) clearly overestimates the river stages with the flows greater than 68.81 m^3/s. Nevertheless, the modeled river stage profiles from Freeman et al. (2000) as well as Järvelä (2004), Baptist et al. (2007) and Whittaker et al. (2015) match the observations under the low flow conditions (Figure 2a-b). When the discharge is low, the roughness of bare river bed is the major contributor of flow resistance because only a small fraction of riparian vegetation is submerged. Therefore, no significant difference is found among these vegetation roughness equations when they are used for simulating low flow conditions.

Besides of the overestimation of Freeman et al. (2000), the river stage profiles predicted by the model with Järvelä (2004), Baptist et al. (2007) and Whittaker et al. (2015) are remarkably similar and match the observations fairly well. The model with other three vegetation roughness equations based on a rigid cylinder analogy, e.g. Huthoff et al. (2007), Cheng (2011) and Luhar and Nepf (2013) also predicts the river profiles as good as Baptist et al. (2007), but these profiles are not necessarily presented in Figure 2. The modeled river stages are slightly lower than the observed data when the upstream flow reached 169.33 m^3/s in January 2011 (Figure 2e). According to the study of Tetra Tech (2013), the high river stage of this flow resulted from a great amount of debris captured during its initial rising limb, given that the study reach had not

experienced flows of this magnitude for years. In addition, modeled river stages deviate from the observations at few locations, for example, the most upper and lower portion of the study reach for Q = 201.62 m^3/s (Figure 2f), this is presumably because spatial distribution of vegetation at these locations in 2011 changed greatly from the 2002's vegetation map used in this study.

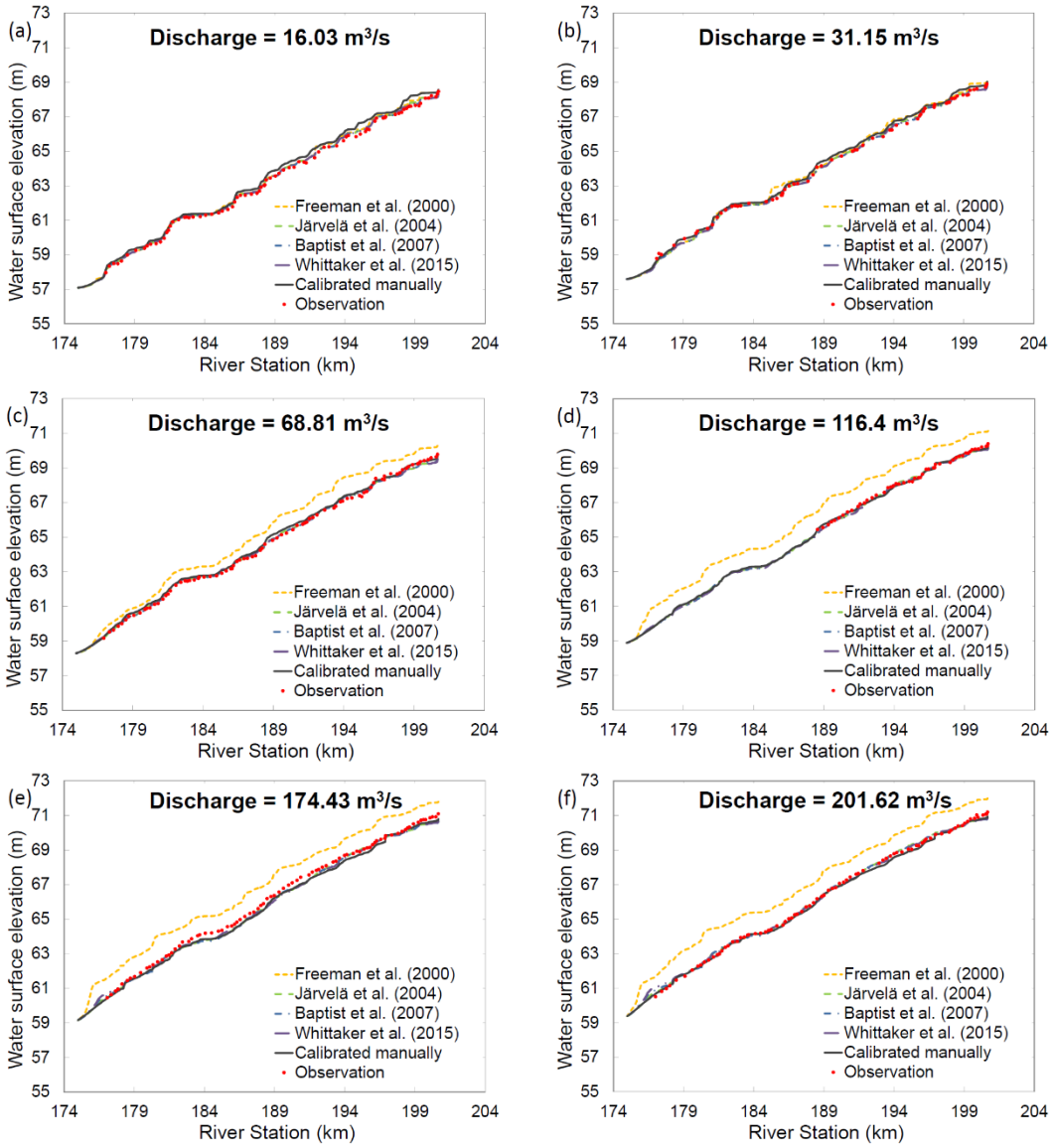

Figure 2. Observed and modeled river stage profiles by using Manning's *n* under six flow scenarios

Compared to the river stage profiles predicted by the HEC-RAS model with manually calibrated *n* values (Tetra Tech, 2013), the models integrated with vegetation roughness computation equations predict river stage profiles more accurately against observed data, particularly for the flows lower than 31.15 m^3/s (Figure 2a-b). The manually calibrated model was able to reproduce observed river stage profiles for high flow conditions, but overestimated river stages under the low flow conditions. The manually calibrated Manning's *n* values were set too high for open water (0.035–0.056), which resulted in the larger error for the low flow conditions. This result demonstrates that the constant Manning's *n* values defined through the model calibration do

not work well for a wide range of flow conditions. The HEC-RAS – RVSM model has the advantage of automatically computing dynamic Manning's *n* values based on the varying flow conditions and vegetation dynamics.

The root mean square errors (RMSEs) between observed and modeled river stages calculated for the seven roughness equations and six flow scenarios are presented in Table 3. The first four equations modeled vegetation as evenly distributed rigid cylinders have almost the same RMSE values. That is because that most trees in the study reach were only partially submerged even under the largest flow rate, these four equations are equivalent for partially submerged trees and shrubs. The water depth increased by 2.44~3.05 m when the river flow rate increased from 16.03 m^3/s to 201.62 m^3/s (Figure 2). This magnitude of flows could only completely submerge the short vegetation at low elevation such as riparian scrub, willow scrub and few mixed riparian low density. Except for the equation of Freeman et al. (2000), the two equations of Järvelä (2004) and Whittaker et al. (2015) that consider vegetation flexibility, have similar RMSE values with these four equations (e.g. Baptist et al., 2007; Huthoff et al., 2007; Cheng, 2011; Luhar and Nepf, 2013) based on a rigid cylinder analogy.

Table 3. RMSEs between observed and modeled river stage profiles by using computed Manning's *n*

Q	16.03m^3/s	31.15m^3/s	68.81m^3/s	116.40m^3/s	174.43m^3/s	201.62m^3/s
Roughness equations	RMSE (m)					
Baptist et al. (2007)	0.106	0.106	0.125	0.113	0.242	0.142
Huthoff et al. (2007)	0.106	0.106	0.125	0.112	0.241	0.141
Cheng (2011)	0.106	0.106	0.125	0.112	0.237	0.139
Luhar and Nepf (2013)	0.106	0.106	0.125	0.112	0.239	0.139
Freeman et al. (2000)	0.194	0.272	0.855	1.106	1.051	1.208
Järvelä (2004) leafy	0.121	0.106	0.137	0.121	0.225	0.126
Whittaker et al. (2015)	0.113	0.110	0.126	0.121	0.231	0.148
Calibrated manually	0.322	0.199	0.164	0.094	0.251	0.207

Model Validation:

The calibrated HEC-RAS –RVSM model was validated using observed river stage hydrographs at DNB in 2011 and SKB in 2017. The RMSE between modeled and observed river stage was used to evaluate the performance of different vegetation roughness equations in hydraulic simulations. Furthermore, a HEC-RAS model originally developed by Tetra Tech (2013) with manually calibrated Manning's *n* values was also used to compare against the HEC-RAS – RVSM model with dynamically computed *n* values. Figure 3 compares HEC-RAS modeled and the observed river stage hydrograph at Donny Bridge gauge (river station 196.9 km) in 2011 and at Skaggs Bridge gauge (river station 182.6 km) in 2017. For both locations, the modeled river stage hydrographs using computed Manning's *n* values by Freeman et al. (2000) are approximately 1 m higher than the observations for the flows greater than 50 m^3/s. The other vegetation roughness equations, in contrast, compute more reasonable Manning's *n* values and produce reasonable river stage predictions under most flow conditions.

The HEC-RAS model performs similarly for the validation period as it does for the calibration period at Donny Bridge gauge in 2011. Compared with manually calibrated Manning's *n*, the model with computed vegetation roughness predicts river stages better matching observed data under the low flow conditions. The two models predict similar river stages under the high flow conditions. Nevertheless, all the vegetation roughness equations except for Freeman et al.

(2000) under-predict Manning's *n* values for the middle flow range, 50-80 m^3/s, resulting in the modeled river stage lower than the observation. The prediction error is probably caused by the fact that the channel contracted sharply at the Donny Bridge gauge and raised the local river stage. The 1D hydraulic model is not able to accurately simulate the river stage change around the complex channel geometry with bridges.

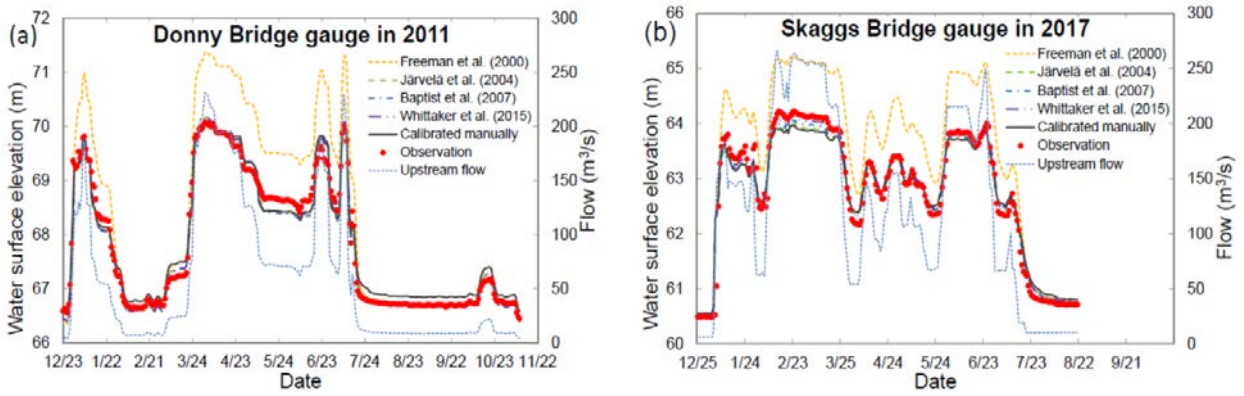

Figure 3. Observed and modeled river stage hydrographs by using computed Manning's *n* at Donny Bridge gauge (a) and Skaggs Bridge gauge (b)

The model validation result at Skaggs Bridge gauge in 2017 reveals that the HEC-RAS –RVSM model is able to predict river stages more accurately for flows higher than the maximum calibration flow (Figure 3b). The simulation of the high flood event (Q = 266 m^3/s) in 2017 demonstrates that as river flow and water level increase, vegetation roughness also increases when most riparian vegetation has not been completely submerged yet. The manually calibrated Manning's *n* values in HEC-RAS can be spatially varying, but usually are constant, therefore, the dynamic change of vegetation roughness with flow conditions cannot be reflected in the hydraulic simulation. The constant Manning's *n* values used for the HEC-RAS model are attributed to too low river stage prediction for the high flood event in 2017. It is worth noting that although the models with dynamically computed Manning's *n* performed better, the predicted river stage for the large flood is still slightly lower than the observation (Figure 3b). This is probably because the flow resistance of leaves and branches was not considered in this study as a result of no survey data about their projected area being available. As the river stage rises to a certain level, plenty of leaves and branches of trees and shrubs start to be submerged, flow resistance caused by the submerged leaves and branches should be taken into account (Västilä and Järvelä, 2014).

According to the above validation results of the two gauges, the HEC-RAS–RVSM model with Whittaker et al. (2015) performed best among the seven roughness equations for trees and shrubs. The RMSE values of the modeled river stage hydrographs at Donny Bridge in 2011 and Skaggs Bridge in 2017 are 0.17 m and 0.19 m, respectively.

Concluding Remarks

Eleven vegetation roughness equations were integrated into the 1D HEC-RAS - RVSM model to compute dynamic roughness coefficients for hydraulic simulations. The model was then applied to a reach of the San Joaquin River for evaluating the performance and applicability of different vegetation roughness equations in 1D hydraulic modeling. The model results demonstrate that the equation of Freeman et al. (2000) clearly overestimates the Manning's *n* values for the flow depth greater than its original experimental flow (1.5m) as a result of the approximately linear

relationship of *n* versus *R* used for emergent vegetation. The equation of Whittaker et al. (2015) considers the reconfiguration of flexible vegetation and uses measured vegetation projected area and is able to predict Manning's *n* values and river stage more accurately than all of the other roughness equations. The four roughness equations modeled vegetation as rigid cylinders produce almost the same results and perform reasonably well in computing Manning's *n* values under the river flows not large enough to completely submerge most riparian vegetation. The equation of Järvelä (2004) includes the impact of velocity on vegetation roughness but uses an indirect metric LAI to represent vegetation projected area, resulting in the similar simulation accuracy with the four equations based on a rigid cylinder analogy.

Compared with manually calibrated Manning's *n* values, the HEC-RAS–RVSM model is able to predict river stage more accurately, particularly under the river flows larger than the maximum calibration flow. The Manning's *n* values computed from these equations reflect their spatial and temporal variations with vegetation distribution and flow conditions. In the study area with the same vegetation type, the vegetation closer to river centerline induces relatively higher Manning's *n* values due to the greater flow depth. Under the similar flow conditions the *n* values of mixed and willow riparian are generally larger than those of cottonwood and riparian scrub because of the higher vegetation density and stiffness. The grassland with shallow flow and low velocity can produce very large *n* values and result in only little conveyance. As flow and river stage increase, the model computed *n* values continuously increases until most riparian vegetation is fully submerged.

Through the application to the San Joaquin River reach, the following suggestions in applying these vegetation roughness equations are given. The equation of Freeman et al. (2000) might be used only for the flow depth within the range of its original experiments. The four rigid vegetation equations can be used to compute dynamic Manning's *n* values for 1D hydraulic modeling when most riparian vegetation is not fully submerged and dominated by trees and shrubs. The projected area of each vegetation community in the foliated and defoliated state needs to be estimated appropriately in order to get the best hydraulic simulation when applying the relatively accurate roughness equation, Whittaker et al. (2015). If vegetation field property data is not available, the equation of Järvelä (2004) that uses the LAI data from remote sensing is a feasible option to compute dynamic Manning's *n* values. Finally, additional data is needed to further evaluate the performance and applicability of the vegetation roughness equations in determining Manning's *n* values for both emergent and submerged vegetation.

Acknowledgments

The work was supported by the U.S. Army Corps of Engineers Ecosystem Management and Restoration Research Program. Mr. Steve Piper, Mr. Mark Jensen, Dr. Junna Wang, and Dr. Blair Greimann are appreciated for providing HEC-RAS support, model integration and San Joaquin River dataset.

References

Augustijn, D. C. M., F. Huthoff, and E. H. v. Velzen. 2008. "Comparison of vegetation roughness descriptions." *Proceedings of River Flow 2008 - Fourth International Conference on Fluvial Hydraulics*, M. S. Altinakar, M. A. Kokpinar, I. Aydin, S. Cokgor, and S. Kirkgoz, eds., Kubaba Congress Department and Travel Services, Çe¿me, Turkey, 343-350.

Baptist, M., V. Babovic, J. U. Rodríguez, M. Keijzer, R. Uittenbogaard, A. Mynett, and A. Verwey. 2007. "On inducing equations for vegetation resistance." *J. Hydraul. Res.*, 45(4),

435-450.
Cheng, N. S. 2011. "Representative roughness height of submerged vegetation." *Water Resear. Res.*, 47(8).
De Doncker, L., P. Troch, R. Verhoeven, K. Bal, P. Meire, and J. Quintelier. 2009. "Determination of the Manning roughness coefficient influenced by vegetation in the river Aa and Biebrza river." *Environ. Fluid Mech.*, 9(5), 549-567.
Fischenich, J. C. 2000. "Resistance due to vegetation." *ERDC TN-EMRRP-SR-07*, US Army Engineer Research and Development Center, Environmental Laboratory, Vicksburg, MS.
Freeman, G. E., W. J. Rahmeyer, and R. R. Copeland. 2000. "Determination of Resistance Due to Shrubs and Woody Vegetation." *ERDC/CHL TR-00-25*, Vicksburg, MS.
Gillihan, T. 2013. "Dynamic Vegetation Roughness in the Riparian Zone." Master of Science, University of New Mexico, Albuquerque, NM.
Hession, W.C., and J.C. Curran. 2013. "The impacts of vegetation on roughness in fluvial systems." In Schroder, J.F., D.R. Butler, and C.R. Hupp (Eds.), *Treatise on Geomorphology*, Vol. 12, 75-93. San Diego, CA: Academic Press.
Hink, V., and R. Ohmart. 1984. "Middle Rio Grande biological survey. Final report to the US Army Corps of Engineers No. DACW47-81-C-0015." Center for Environmental Studies, Arizona State University Tempe, AZ.
Holland, R. F. 1986. "Preliminary descriptions of the terrestrial natural communities of CA."
Huthoff, F., D. Augustijn, and S. J. Hulscher. 2007. "Analytical solution of the depth-averaged flow velocity in case of submerged rigid cylindrical vegetation." *Water Resear. Res.*, 43(6).
Järvelä, J. 2004. "Determination of flow resistance caused by non-submerged woody vegetation." *Int. J. River Basin Manage.*, 2(1), 61-70.
Jalonen, J., J. Järvelä, and J. Aberle. 2013. "Leaf area index as vegetation density measure for hydraulic analyses." *J. Hydraul. Eng.*, 139(5), 461-469.
Kouwen, N. 1988. "Field estimation of the biomechanical properties of grass." *J. Hydraul. Res.*, 26(5), 559-568.
Kouwen, N., and M. Fathi-Moghadam. 2000. "Friction factors for coniferous trees along rivers." *J. Hydraul. Eng.*, 126(10), 732-740.
Kouwen, N., and R. M. Li. 1980. "Biomechanics of vegetative channel linings." *J. Hydraul. Div.*, 106(HY6), 1085-1103.
Luhar, M., and H. M. Nepf. 2013. "From the blade scale to the reach scale: A characterization of aquatic vegetative drag." *Adv. Water Resour.*, 51, 305-316.
Moise, G. W., and B. Hendrickson. 2002. "Riparian vegetation of the San Joaquin River." Department of Water Resources, San Joaquin District, Environmental Services Section, Fresno, CA.
Naiman, R. J., H. Decamps, and M. E. McClain. 2005. *Riparia: ecology, conservation, and management of streamside communities*, Academic Press.
Stone, M. C., L. Chen, K. S. McKay, J. Goreham, K. Acharya, J. C. Fischenich, and A. B. Stone. 2013. "Bending of submerged woody riparian vegetation as a function of hydraulic flow conditions." *River Res. Appl.*, 29(2), 195-205.
Tetra Tech. 2013. "San Joaquin River and Bypass System 1-D Steady State HEC-RAS Model Documentation." Fort Collins, CO.
Västilä, K., and J. Järvelä. 2014. "Modeling the flow resistance of woody vegetation using physically based properties of the foliage and stem." *Water Resear. Res.*, 50(1), 229-245.
Whittaker, P., C. A. Wilson, and J. Aberle. 2015. "An improved Cauchy number approach for predicting the drag and reconfiguration of flexible vegetation." *Adv. Water Resour.*, 83, 28-35.
Wu, W. 2007. *Computational river dynamics*, CRC Press.
Zhang, Z., B.E. Johnson, and B.P. Greimann. 2019. HEC-RAS–RVSM (riparian vegetation simulation module), *ERDC TN-EMRRP-SR-X*. Vicksburg, MS.